

SIMULATION OF SALT WATER INTRUSION

Kenzi Karasaki¹⁾, Kazumasa Ito²⁾, Keisuke Maekawa³⁾

¹⁾ Lawrence Berkeley National Laboratory
 1 Cyclotron Rd., MS 90-1116,
 Berkeley, CA, 94720, USA
 kkarasaki@lbl.gov

²⁾ National Institute of Advanced Industrial Science and Technology
 Tsukuba Central 7, 1-1, Higashi 1-Chome, Tsukuba-shi, Ibaraki-ken,
 305-8567 Japan
 kazumasa-ito@aist.go.jp

³⁾ Japan Atomic Energy Agency
 4-33, Muramatsu, Tokai-mura
 Naka-gun, Ibaraki, 319-1194 Japan
 maekawa.keisuke@jaea.go.jp

ABSTRACT

We have modeled laboratory experiments of saltwater intrusion using TOUGH2/EOS7. Matching laboratory and simulation results turned out to be quite challenging partly because of numerical dispersion and partly because the experiments were not very well controlled. Specifically, the model is not able to reproduce the transient salt concentration profile observed in the laboratory very well. In order to understand better the effects of numerical dispersion, we simulated the so-called Henry problem, in which a large dispersion coefficient is assumed, resulting in a wide transition zone between freshwater and saltwater. Henry attributed the large dispersion to the effect of tidally induced motion. We imposed a time-varying sinusoidal boundary condition to see if a large transition zone can be created without explicitly modeling dispersion. However, for the parameters used we were not able to do so. It is still plausible that a wide transition zone is caused by formation heterogeneity and transient effects. Nonetheless, we question the validity of the use of a large dispersion coefficient where the velocity is very low, or where the flow is in the opposite direction of the concentration gradient.

INTRODUCTION

Several countries are considering constructing a nuclear waste repository near the seashore. However, bentonite, which is one of the favored materials to be

used for backfilling boreholes and excavations, may not swell in saltwater as it does in freshwater, and therefore may not provide a reliable seal. Furthermore, saltwater at depth is thought to be stagnant but not much study has been conducted so far. Therefore, it is important to understand the dynamics of the interaction between freshwater and saltwater for assessing the long term safety of a repository. In the present paper we outline the results of numerical simulations of saltwater intrusion into a freshwater body.

LABORATORY EXPERIMENT

Japan Nuclear Energy Agency (JAEA) has been conducting a saltwater intrusion experiment in the laboratory using glass beads and colored saltwater in

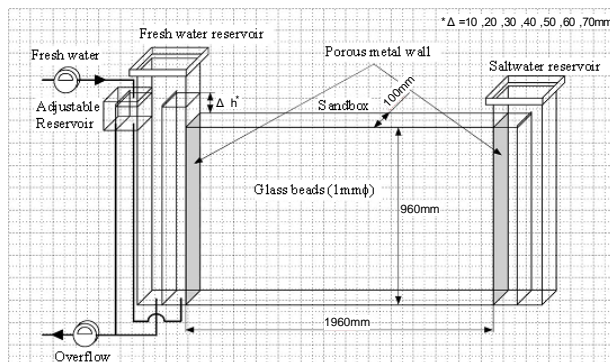


Figure 1: Schematic of the saltwater intrusion visualization experiment



Figure 2: Saltwater positions at 90 minutes after the start of experiment with $\Delta h = 10\text{mm}$ from the (a) first and (b) second experiment

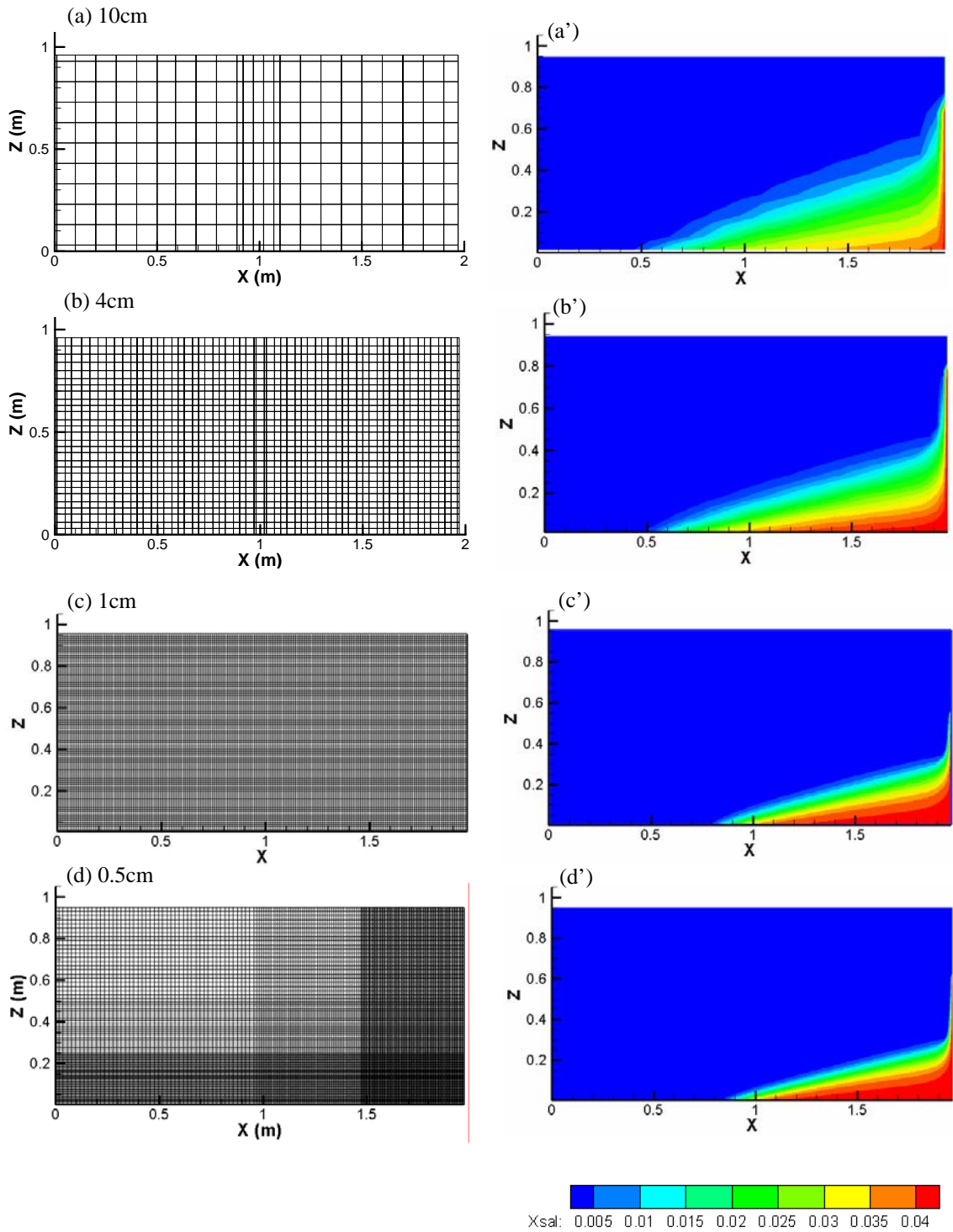


Figure 3: Simulation results of the saltwater intrusion experiment with various grid spacing: (a) 10cm, (b) 4cm (c) 1cm, (d): 0.5cm (partial). The total node numbers are: 250, 1,680, 18,715, and 19,600, respectively. The case shown is for $\Delta h=10\text{mm}$ at $t = 90\text{min}$.

a sandbox with a transparent face plate to allow for visualization (Figure 1). The dimension of the apparatus is 0.96m x 1.96m x 0.1m. The hydraulic conductivity of the glass beads was measured to be 1.14×10^{-2} m/s. Porous metal plates were used on both sides to hold the glass beads in place. The hydraulic conductivity of the porous metal was measured to be 1.29×10^{-5} m/s, which is three orders of magnitude smaller than that of the glass beads.

A reservoir tank filled with degassed freshwater is attached on the left side. The height of the freshwater column is made adjustable so that the fixed head boundary condition on the left side can be varied. A saltwater reservoir is attached on the right side. The height of the saltwater column is fixed at 140mm above the top of the sandbox, which is sealed to ensure the saturated and confined condition.

The glass beads are initially saturated with degassed freshwater. The experiment is initiated by raising the water column by Δh mm and supplying saltwater in the right reservoir. Subsequently the fresh water flows into the sandbox from the left and the red-colored saltwater encroaches from the right side. Due to the difference in density, saltwater flows toward the bottom of the model while freshwater flows toward the top. The encroachment of the saltwater wedge was monitored by conductivity sensors embedded in the back of the sandbox. The images of the advancing saltwater were captured by a digital camera every 30 minutes. Unfortunately, none of the experiment appears to have reached a steady state due to time constraint.

Two series of experiments, where Δh was varied from 10mm to 70mm, were conducted 6 months apart, which produced puzzlingly different results. Figure 2 shows the saltwater positions from the two separate experiments at $t = 90$ minutes for the same $\Delta h = 10$ mm case. One possible explanation is that the permeability of the porous metal had degraded in time. We suspect that the experiment was very sensitive to the low-permeability porous metal plates on both ends, whose permeability is nearly three orders of magnitude lower than that of the glass beads.

NUMERICAL SIMULATIONS

We have simulated the saltwater intrusion experiment using TOUGH2/EOS7 (Pruess, 1991; Pruess et al., 1999). The experiment is modeled in a 2-D domain, which is discretized with various grid spacing from 10cm to 0.5cm. Figure 3 compares the simulation results with various discretization levels at $t = 90$ minutes for the $\Delta h = 10$ mm case, which corresponds to Figure 2. Because no molecular diffusion or hydrodynamic dispersion is implemented in the model, the transition area between the blue

freshwater and the red saltwater is strictly due to numerical dispersion. As can be seen from the figure, the denser the mesh is, the narrower the transition zone is, with less numerical dispersion. With less than 1cm grid interval, the simulation result appears relatively close to that of the experiment. The simulation matches better with the experiment in the second series for the $\Delta h = 10$ mm case. However, although not shown, for other cases including $\Delta h =$

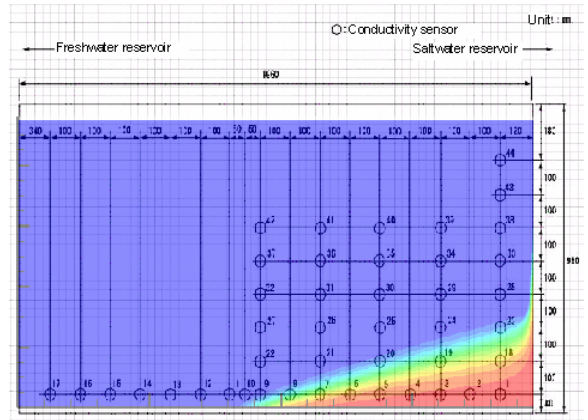


Figure 4: Monitoring points that are equipped with an electric conductivity sensor. A simulation result is superimposed.

50mm and 70mm, the simulation results are closer to those of the first series of experiments.

Figure 4 shows the location of the electrical conductivity sensors for monitoring the saltwater concentration profile. The superimposed figure is a simulated image of the saltwater concentration profile from Figure 3(c'). Figure 5 is a time vs. concentration plot at Probes 1-11 shown in Figure 4 for the $\Delta h = 10$ mm case. As can be seen from the figure, the saltwater front in the experiment is

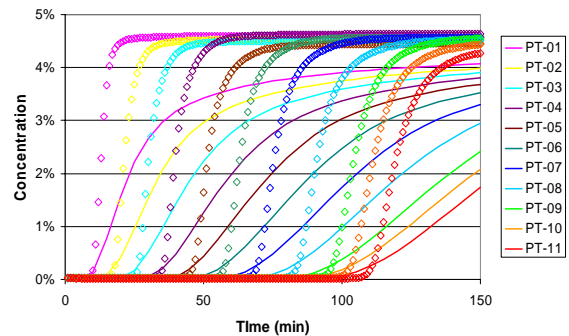


Figure 5: Time vs. concentration plot for monitoring points 1 ~ 11 in Figure 4. The solid lines are simulation results with 1cm grid spacing and the symbols denote the measured data.

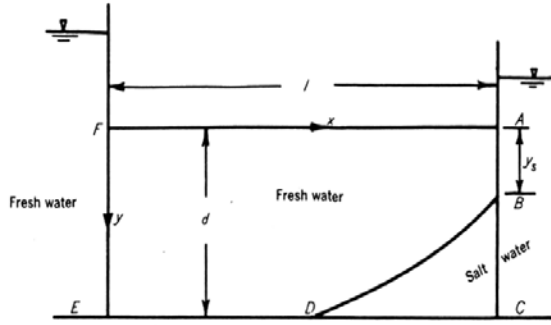


Figure 6: The Henry Problem (After Cooper et al., 1964)

significantly steeper than that of the simulation with a 1cm grid spacing. Although the arrival times are matched relatively well, the simulation significantly under-predicts the concentration and over-predicts the width of the front, particularly for the higher numbered probes that are located downstream.

Here a question arises: How fine should one discretize the grid to achieve enough accuracy? If the actual dispersion is similar to or greater than the numerical dispersion, the grid spacing can be determined by the available computational resource. Otherwise, a caution must be exercised when using a conventional finite difference scheme. In the case studied, even with the very fine grid spacing of 1cm, we could not satisfactorily reduce the numerical dispersion. It may be necessary to employ such schemes as the random choice (Chorin, 1977; Lai, 1985), LTVD (Oldenburg and Pruess, 2000), the method of characteristics (Konikow et al., 1997), the adaptive Eulerian-Lagrangian scheme (Neuman, 1981; Cheng et al., 1984; Ijiri and Karasaki, 1994), the multigrid method (Li et al., 2000) and others.

HENRY PROBLEM

Henry (1964) presented a semi-analytical solution to the saltwater intrusion problem shown in Figure 6, which was followed by several others (Frind, 1982;

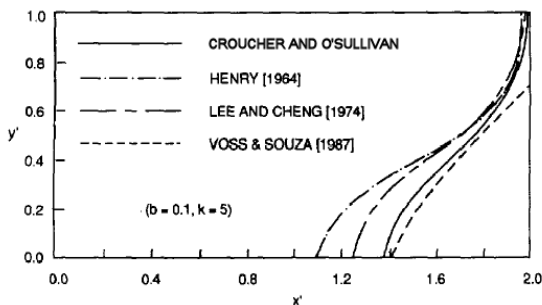


Figure 7: Comparison of the position of the $c = 0.5$ contour (After Croucher and O'Sullivan, 1995)

Voss and Souza, 1987; Croucher and O'Sullivan, 1995; Oldenburg and Pruess, 1995; Held et al., 2005). It appears that among the past works, there are some discrepancies in the results (Figure 7). Nonetheless, they all assume a constant, large dispersion coefficient that results in a wide transition zone between the freshwater and the saltwater. Henry had attributed the large dispersion to the varying discharge rate and the transient tidal effects.

Although the experiment outlined in the previous section resembles the Henry problem, they are not quite the same due to the presence of the low permeability porous walls on both sides of the sandbox. Much of the head drop occurs across the porous metal plates, which significantly influences the outcome. This explains the fact that the saltwater wedge observed in the experiment is more acute than that predicted by the sharp interface solution (Cooper et al, 1964; Huyakorn et al, 1996). Nonetheless, only very little dispersion is observed in the experiment.

We simulated the saltwater intrusion again, this time without the low permeability walls in anticipation of re-running the actual laboratory experiment without them. Although many of the past works assigned a fixed flow rate boundary condition on the left, we assign a fixed head boundary condition to be consistent with the experiment.

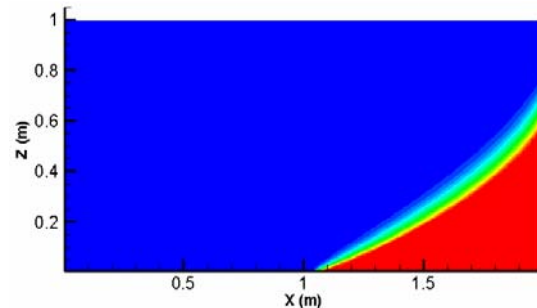


Figure 8: Simulated saltwater wedge for $\Delta h = 40 \text{ mm}$, $D = 1 \times 10^{-9} \text{ m}^2/\text{s}$

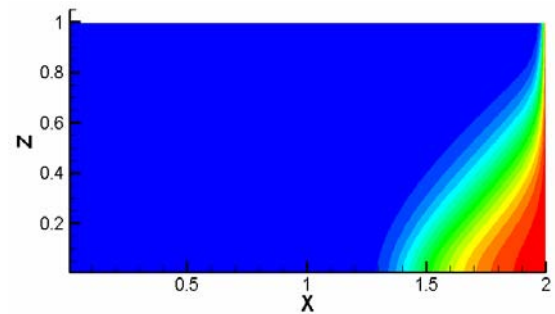


Figure 9: Simulated saltwater wedge, for $\Delta h = 40 \text{ mm}$, $D = 6.6 \times 10^{-6} \text{ m}^2/\text{s}$

Figure 8 shows the simulated saltwater wedge profile at the steady state. Here we use a molecular diffusion coefficient of $1 \times 10^{-9} \text{ m}^2/\text{s}$. It turns out that setting the coefficient to zero makes no visible difference. The profile shows less numerical dispersion than the simulation of the experiment, in which there was a large permeability contrast between the low permeability porous metal and the glass beads. This leads us to suspect that the Although the actual experiment has not been run yet, judging from the previous experience we expect the results will show a very sharp interface.

We then simulated the same problem using a large diffusion coefficient ($6.6 \times 10^{-6} \text{ m}^2/\text{s}$), which is equivalent to assuming a constant (independent of velocity) dispersion coefficient that is consistent with the past works. We now obtain a wide transition zone,

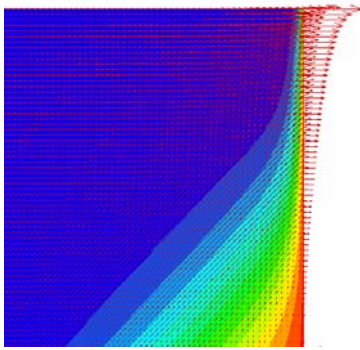


Figure 10: Enlarged upper right hand corner of Figure 9. Arrows indicate the flow velocity at each node.

a blunt leading edge, and a shorter encroachment distance (Figure 9) similar to those seen in Figure 7. Because the freshwater inlet boundary condition is different (constant head vs. constant flux), no exact match is expected.

The use of a large constant dispersion coefficient (i.e. diffusion coefficient) to model hydrodynamic dispersion, however, is questionable. Figure 10 shows the enlarged upper right corner of Figure 9 superimposed with red arrows to indicate the flow velocity. As can be seen in the figure, dispersion is taking place in the opposite direction of the flow of the freshwater. Of course this is expected because of the large diffusion (dispersion) coefficient assigned in the model. However, it is unphysical for hydrodynamic dispersion to occur in the opposite direction of flow. The same argument applies to the dispersion at the freshwater-saltwater interface, where the saltwater is essentially stagnant and the freshwater is flowing in the opposite direction of the concentration gradient.

Notwithstanding, a large dispersion can only come from hydrodynamic dispersion. We assigned a time-varying sinusoidal head boundary condition on either side of the boundary to see if a wide transition zone can be created with a diffusion coefficient of $10^{-9} \text{ m}^2/\text{s}$. We varied the head $40 \text{ mm} \pm 5 \text{ mm}$ with frequencies from $1/7.5 \text{ min}$ to $1/750 \text{ min}$. However for the parameters used, we were not able to create a wide dispersion zone. A wedge identical to that shown in Figure 8 shifted back and forth maintaining the sharp interface. Although Held et al. (2005) concluded that the steady state saltwater distribution is not very sensitive to heterogeneities and longitudinal dispersion, it is still plausible that the right combination of heterogeneity and head variation may create a wide transition zone.

CONCLUSIONS

The present study underscores the importance of using caution when choosing the mesh size of a given problem. One should not determine the size arbitrarily or by convenience. Even for a deceptively simple problem like saltwater intrusion, where advective transport process is involved; an ordinary finite difference scheme can suffer significant numerical dispersion. It is prudent to use the densest mesh one can afford and still be wary of potential inaccuracy.

Care must be used when using a large constant dispersion coefficient to model dispersive phenomena. It is unphysical when the advective flow velocity is large but in the opposite direction of the concentration gradient.

ACKNOWLEDGMENT

This work was conducted under Contract No. DE_AC03-76SF00098. The authors would like to thank Curt Oldenburg for his useful suggestions.

REFERENCES

- Cheng, R.T., Casulli, V., and Milford, S.N., Eulerian-Lagrangian solution of the convection-dispersion equation in natural coordinates. *Water Resour. Res.*, 20(7), pp.944-952, 1984.
- Chorin, A.J., Random choice method with application to reacting gas flow, *J. Comp. Phys.*, v25, pp.253-272, 1977.
- Cooper, et al., Sea water in coastal aquifers, *U.S. Geol Surv. Water Supply Pap.*, 1613-C, p.84,1964.
- Croucher, A. E. and M. J. O'Sullivan, The Henry problem for saltwater intrusion, *Water Resour. Res.*, 31(7), pp.1809-1814, 1995.
- Frind; E. O., Simulation of long-term transient density-dependent transport in groundwater, *Adv. Water Resour.*, 5, 73-88, 1982.

- Henry, H. R., Effects of dispersion on salt encroachment in coastal aquifers, *U.S. Geol Surv. Water Supply Pap.*, 1613-C, C71-C84, 1964.
- Held, R., S. Attinger, W. Kinzelbach, Homogenization and effective parameters for the Henry problem in heterogeneous formations, *Water Resour. Res.*, 41, W11420, 2005.
- Huyakorn, P.S., Y.S. Wu, and N.S. Park, Multiphase approach to the numerical solution of a sharp interface saltwater intrusion problem, *Water Resour. Res.*, 32(1), pp.93-102, 1996.
- Ijiri, Y, and K. Karasaki, A Lagrangian-Eulerian Finite Element Method with Adaptive Gridding for Advection-Dispersion Problems, in *Proceedings of International Conference on Computational Methods in Water Resources*, Heidelberg, Germany, 1994.
- Konikow, L. F., W. E. Sanford, and P. J. Campbell, Constant-concentration boundary condition: Lessons from the HYDROCOIN variable-density groundwater benchmark problem, *Water Resour. Res.*, 33(10), pp.2253-2261, 1997.
- Lai, C-H.. Mathematical models of thermal and chemical transport in geologic media (Ph.D. thesis). Lawrence Berkeley Laboratory Report LBL-21171, 1985.
- Lee, C., and R. Cheng, On seawater encroachment in coastal aquifers, *Water Resour. Res.*, 10(5), pp.1039-1043, 1974.
- Li, M.-H., H.-P. Cheng, and G. T. Yeh, Solving 3D subsurface flow and transport with adaptive multigrid, *J. Hydrol. Eng.*, 5, pp.75- 81, 2000.
- Neuman, S.P., An Eulerian Lagrangian numerical scheme for the dispersion-convection equation using conjugate space-time grids. *J. Comput. Phys.*, 41, pp.270-294, 1981.
- Oldenburg, C.M. and K. Pruess, Dispersive transport dynamics in a strongly coupled groundwater-brine flow system, *Water Resour. Res.*, 31(2), pp.289-302, 1995.
- Oldenburg, C. M., K. Pruess, Simulation of propagating fronts in geothermal reservoirs with the implicit Leonard total variation diminishing scheme, *Geothermics* 29, pp.1-25, 2000.
- Pruess, K., C. Oldenburg, and George Moridis, *TOUGH2 User's Guide*, Lawrence Berkeley National Laboratory Report, LBNL-43134, 1999.
- Pruess, K. EOS7, *An Equation-of-State Module for the TOUGH2 Simulator for Two-Phase Flow of Saline Water and Air*, Lawrence Berkeley Laboratory Report, LBL-31114, Berkeley, CA, 1991.
- Voss, C. I., and W. R. Souza, Variable density flow and solute transport simulation of regional aquifers containing a narrow freshwater-salt water transition zone, *Water Resour. Res.*, 23(10), pp.1851-1866, 1987.